Computational Study of the "Stable" Bis(amino)silylene Reaction with Halomethanes. A Radical or Concerted Mechanism?

Hyun Joo and Michael L. McKee*

Department of Chemistry and Biochemistry, Auburn University, Auburn, Alabama 36849

Received: December 6, 2004; In Final Form: February 26, 2005

The reaction of bis(amino)silylene with XCH_3, X = Cl, Br, I, has been studied computationally using DFT with flexible basis sets. A radical process where a halogen atom is abstracted from halomethane is predicted to be much more favorable than oxidative addition of the halomethane to the divalent silicon center. A chain mechanism is proposed that consists of a chain-initiation step (halogen abstraction) followed by competing chain-propagation steps. In one branch, the methyl-substituted bis(amino)silylene abstracts a halogen from XCH_3 to form an observed product (the 1:1 adduct), releasing a methyl radical. In the other branch, the methyl-substituted bis(amino)silylene is intercepted by another bis(amino)silylene, which, in turn, can abstract a halogen from XCH_3 to form the other observed product (the 2:1 adduct) and release a methyl radical. In the series, XCH_3, X = Cl, Br, and I, we predict an increase of the 1:1 adduct-producing pathway over the 2:1 adduct-producing pathway, which is consistent with experimental observations. The reactivity of bis(amino)-silylene indicates a greater similarity to disilene rather than to previously suggested phosphines.

Introduction

The first report of the isolation of a stable silylene, *N,N′*-di-*tert*-butyl-1,3-diaza-2-silacyclopent-4-en-2-ylidene, **1**, in 1994[1] resulted in a flurry of publications investigating its chemical and physical properties. At the forefront of the research was the origin of its stability. Both theoretical[2−10] and experimental[8−12] work have concurred that π-electron donation from the α-substituent to the formally empty silicon p orbital and possible aromaticity of the 6-π electron ring are the main factors causing the divalent silicon species to be stabilized.

In addition, there has been an active interest in the reactivity of **1** and related silylenes.[12−18] A divalent silylene, like the isolelectronic divalent carbene,[19] can be a Lewis acid or a Lewis base by virtue of its low lying vacant p orbital (Lewis acid) and its nonbonding electron pair (Lewis base). It is now well established that acyclic silylenes and cyclic alkyl silylenes behave as Lewis acids.[7a,12] On the other hand, cyclic bis(amino)-silylenes can act as Lewis bases by donating the nonbonding electron pair on the silicon atom as in silylene-metal complexes,[14−18] or in Arduengo carbenes (1,3-diimidazol-2-ylidene).[19]

As shown in Scheme 1, π conjugation increases the electron population of the empty p orbital on the Si atom, which leads to lower acidity and higher basicity. This can account for the different reactivities of the two types of silylenes, dialkylsilylenes (Lewis acids) and bis(amino)silylenes (Lewis bases).

A number of reactions utilize the electron donicity of **1**, and are well understood.[13−17] However, few examples can be found for the reaction of **1** with Lewis bases. Recently, reactions of silylenes with halocarbons were reported.[18,20−22] The reactions of dialkylsilylene, 2,2,5,5-tetrakis(trimethylsilyl)silacyclopentane-1,1-diyl, **2**, with halomethanes were studied by Ishida et al.[20] The reactions of **2** with CCl_4 and $CHCl_3$ gave dichlorosilane by a radical mechanism. Methyl iodide also reacts with **2** to give a single insertion product. However, the reaction with CH_2Cl_2 gave double insertion products in which two Si atoms

SCHEME 1

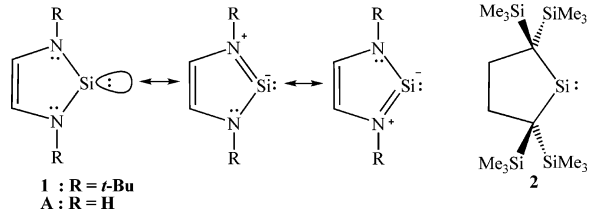

SCHEME 2

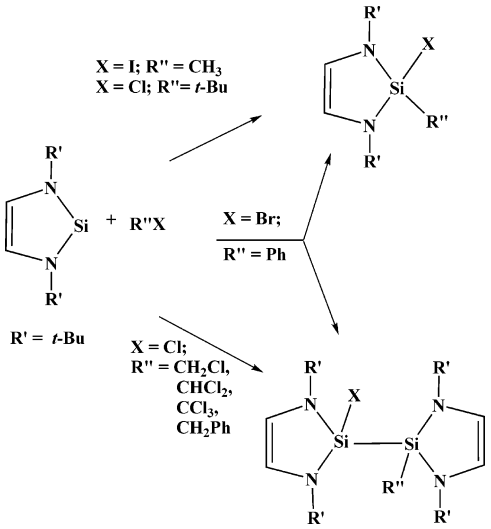

are bonded to a carbon atom. The authors[20] suggested that the activation of the C−Cl bond by silylene complexation would facilitate the nucleophilic attack of another silylene and proposed a Lewis acid-Lewis base reaction mechanism via an acid−base complex. Similarly, the reactions of **1** with halomethanes (Scheme 2) were reported by West and co-workers.[18,21,22] The reaction between **1** and ICH_3 was reported to give a 1:1 adduct as exclusive product, whereas chlorocarbons, except for *t*-BuCl,

10.1021/jp044458p CCC: $30.25
Published on Web 04/02/2005

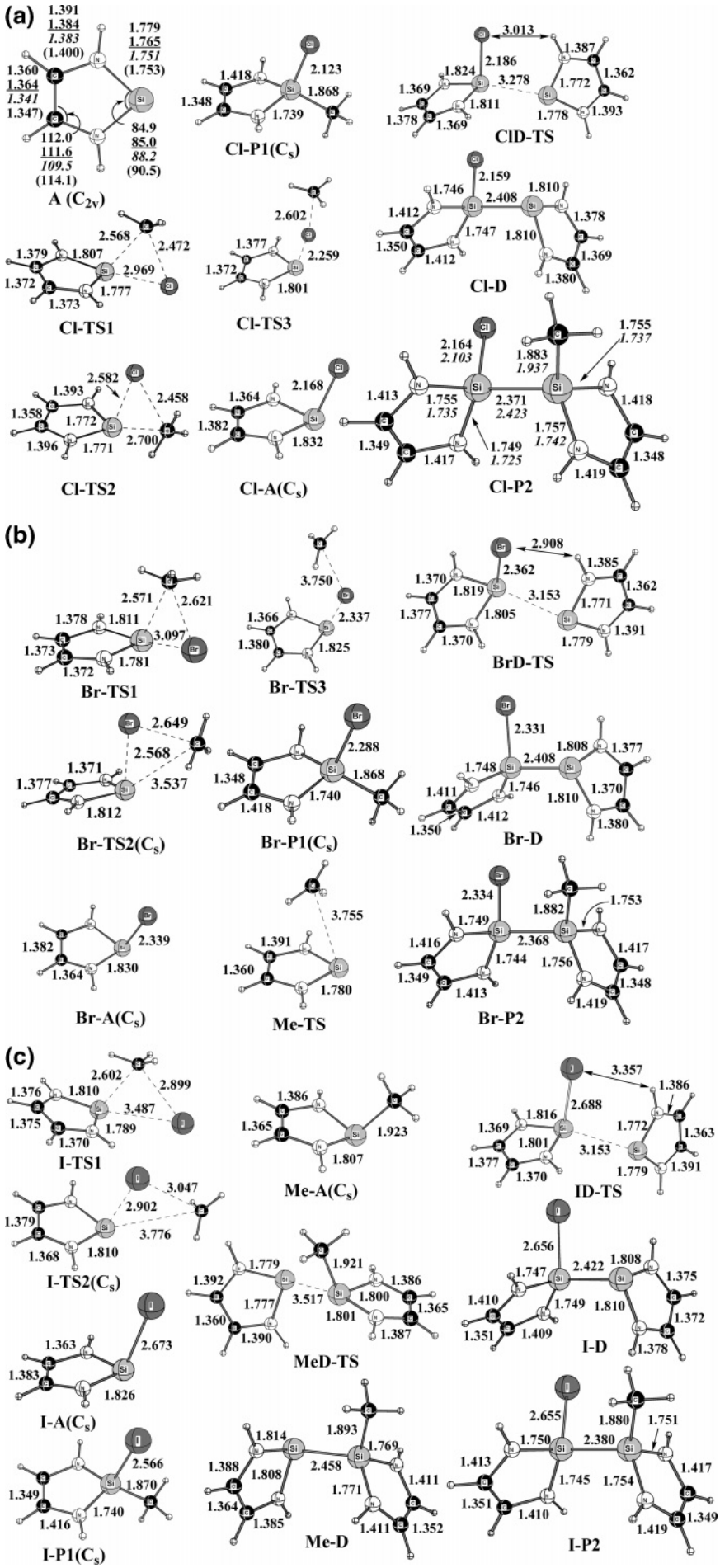
(a)
A (C_{2v})
Cl-P1(C_s)
ClD-TS
Cl-TS1
Cl-TS3
Cl-D
Cl-TS2
Cl-A(C_s)
Cl-P2
(b)
Br-TS1
Br-TS3
BrD-TS
Br-TS2(C_s)
Br-P1(C_s)
Br-D
Br-A(C_s)
Me-TS
Br-P2
(c)
I-TS1
Me-A(C_s)
ID-TS
I-TS2(C_s)
MeD-TS
I-D
I-A(C_s)
Me-D
I-P1(C_s)
I-P2

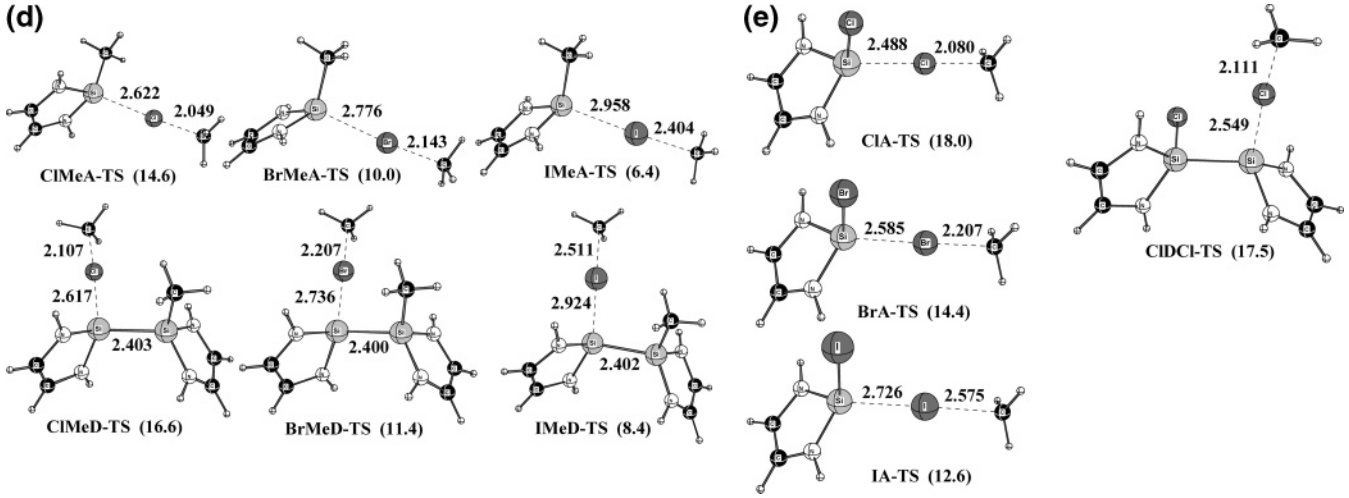

Figure 1. Geometries optimized at B3LYP/6-31+G(d) level where bond lengths are in Å, angles are in degrees, and Schönflies symbols are given in parentheses. (a) Geometrical parameters for stationary points in the reaction of **A** with $ClCH_3$. The geometry of **A** is compared with MP2/6-311G(d)[2b] (underlined); with **1** by gas-phase electron diffraction[1] in parentheses; and with **1** by X-ray diffraction[32] (italicized). The geometry of **Cl**−**P2** is compared with X-ray diffraction[22] where the *t*-Bu groups have replaced the hydrogens on nitrogen. (b) Geometrical parameters of stationary points in the reaction of **A** with $BrCH_3$. (c) Geometrical parameters of stationary points in the reaction of **A** with ICH_3. (d) Geometrical parameters of transition states in the reaction of **Me**−**A** with XCH_3 (**XMeA-TS**) and in the reaction of **Me**−**D** with XCH_3 (**XMeD-TS**). Free energies in kcal/mol are given in parentheses with respect to reactants. (e) Geometrical parameters of transition states in the reaction of **X**−**A** with XCH_3 (**XA-TS**) and in the reaction of **Cl**−**D** with $ClCH_3$ (**ClDCl-TS**). Free energies in kcal/mol are given in parentheses with respect to reactants.

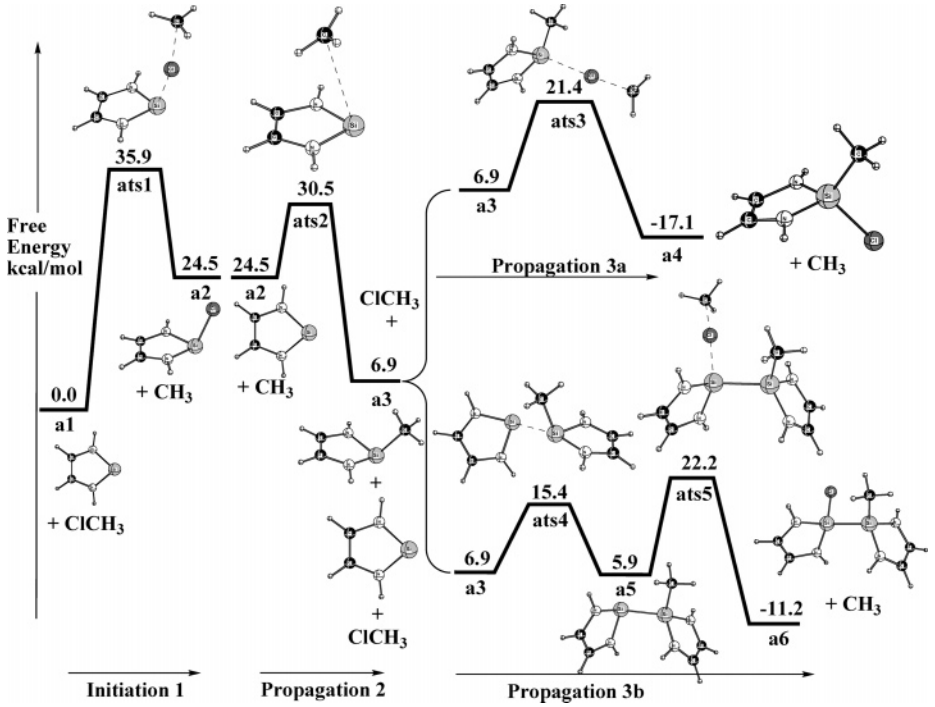

Figure 2. Schematic reaction free energy profile is presented for the reaction of **A** with $ClCH_3$ at the B3LYP/LBS//B3LYP/SBS level. The figure is divided into an initiation step (1), a common propagation step (2), and two competing propagation steps (3a and 3b). The initiation step produces a CH_3 radical, which, in turn, adds to another bis(amino)silylene. The free energy of **Cl**−**A** + CH_3 and CH_3 + **Me**−**A** are shown at the same free energy so that free energies over the entire reaction can be compared. The entire list of species represented by the label (e.g., **a2**) is given in Table 3.

reacted with **1** to give a 2:1 adduct. Interestingly, reaction with bromobenzene gave mixed products of the 1:1 and 2:1 adducts (Scheme 2). Further investigation showed that the proportion of product yields, 1:1 and/or 2:1 adducts, changed depending upon the ratio of the reactants. Also, increasing the bromobenzene ratio led to a higher proportion of 1:1 adduct with exclusively 1:1 adduct after four equivalences of bromobenzene. From these observations, a radical mechanism was suggested for the formation of the 1:1 adducts with ICH_3, but a 1,2-shift mechanism with bromobenzene and *t*-BuCl via a 1:1 intermediate complex. For chlorocarbons, a halophilic mechanism via a 1,3-shift from a 2:1 intermediate complex was proposed. Both silylenes, **1** and **2**, show similar trends of reactivities toward halomethanes, even though they have completely different chemical properties.

Recently theoretical studies on the mechanism of halophilic reactions of silylene **A** (Scheme 1) with $ClCH_3$, $CHCl_3$ and $CHBr_3$ were reported at the B3LYP/6-31G* level.[23] The author suggested that the reactions follow the general pathway: insertion of silylene into a halogen−carbon bond followed by dimerization with another silylene to form the final 2:1 reaction product. However, the reported results cannot completely

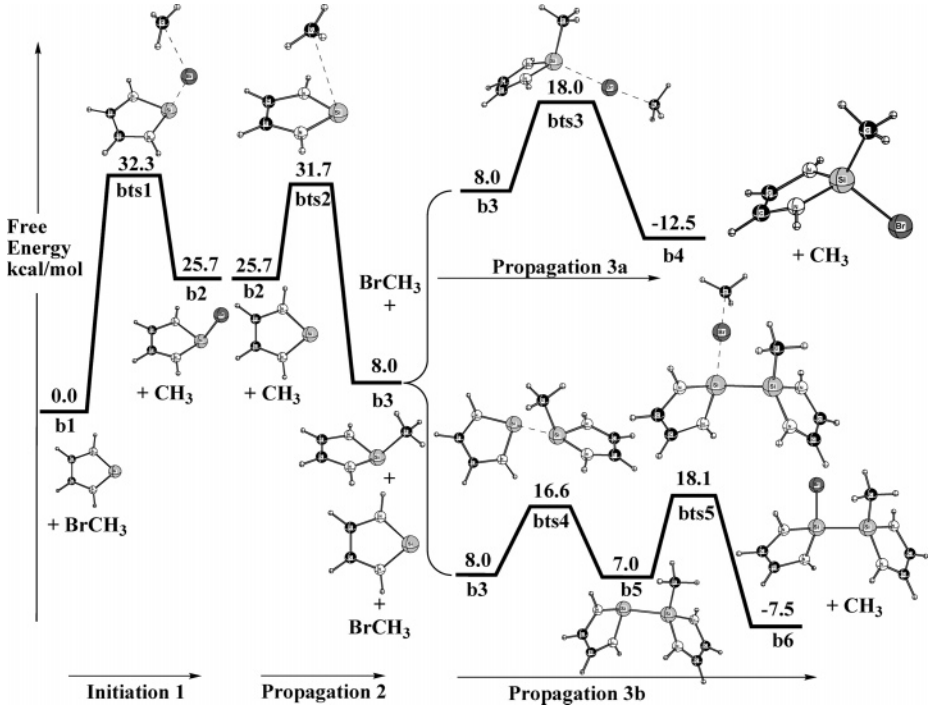

Figure 3. Schematic reaction free energy profile is presented for the reaction of **A** with $BrCH_3$ at the B3LYP/LBS//B3LYP/SBS level.

account for the experimental observations. If the disilane product (2:1 adduct) were formed via initial insertion into Si−X bond of the 1:1 product, the 1:1 product should be observed in the reaction of silylene **1** with a 100-fold excess of $CHCl_3$ as is the case in the reaction with bromobenzene.[22] Furthermore, the possibility of radical involvement was excluded in the study, because only restricted DFT calculations were performed.[23] Therefore, we felt that it is necessary to reinvestigate the reaction of bis(amino)silylene (**A**) with halomethanes to consider the radical mechanism.

Computational Details

Possible reactions of silylene **A** with XCH_3 (X = Cl, Br, I) were examined by using density functional theory[24] implemented in the Gaussian03 program.[25] The hybrid B3LYP combination of exchange and correlation functionals[26] was utilized throughout this study. Geometry optimizations of all stationary points were performed with a 6-31+G(d) basis set for H, C, N, Si, Cl and Br and with a standard LanL2DZ[27] effective core potential (ECP) and basis set for I (Figure 1). At each stationary point, vibrational frequencies were calculated to confirm whether it was a minimum (no imaginary frequencies) or transition state (one imaginary frequency). At every transition state, the transition vector was animated with the Molden program,[28] and if necessary, the intrinsic reaction coordinate (IRC)[29] was computed to connect the corresponding minima. To obtain a better energetic description of the reaction profile, single-point calculations were performed with a larger 6-311++G(2df,p) basis set for all atoms except for I, for which the SDD[30] ECP and basis set were used. Thermodynamic corrections to 298 K, zero-point vibrational energy corrections (ZPC), heat capacity corrections (C_p), and entropy corrections (ΔS) obtained at the B3LYP/6-31+G(d)+LanL2DZ level were applied to single-point energies at the B3LYP/6-311++G(2df,p)+SDD level. The reaction profiles were constructed on the basis of relative free energy at 298 K (Figures 2−4). For convenience, "SBS" will be used to denote the 6-31+G(d)+LanL2DZ basis set and "LBS" to denote the 6-311++G(2df,p)+SDD basis set. The transition states on the singlet PES were tested to determine whether a spin broken-symmetry solution was lower in energy. If so, the transition state was reoptimized with the spin broken-symmetry method. These structures are tabulated in Table 1 (**Cl**−**TS3**, **Br**−**TS2**, **Br**−**TS3**, **I**−**TS2**) with the $\langle S^2 \rangle$ expectation value. A notation scheme is used in the text, Figures, and Tables for the various structures where "**X**" is the halogen (**Cl**, **Br**, or **I**), "**A**" is the cyclic bis(amino)silylene, "**D**" stands for two cyclic silylene units bonded with a Si−Si bond, and "**P**" stands for a product.

Natural population analysis (NPA) was carried out on the important radical intermediates at the UB3LYP/SBS level by utilizing the NBO program[31] implemented in Gaussian to explain the different reactivity of silylene toward halomethanes. In addition, Si−CH_3 and Si−X bond enthalpies were determined in **X**−**P1** (Figure 1; X = Cl, Br, I) and compared with X−CH_3 bond enthalpies.

Result and Discussion

Bond lengths and bond angles of **A** optimized at the B3LYP/6-31+G(d) level are in good agreement with those at the MP2/6-311G(d) level[2b] and also agree with those determined by gas-phase electron-diffraction[1] and solid-state X-ray diffraction[32] of the *t*-Bu derivative, **1** (Figure 1a). The slightly longer Si−N bond lengths in **A** than in **1** can be rationalized by greater electron donation from the *t*-Bu group in **1**. The possible radical intermediates, **X**−**A** (X = Cl, Br, I) and **Me**−**A**, show interesting characteristics. Because the 4n+2 π-electron system is interrupted by the addition of a halogen radical in **X**−**A** or a methyl radical in **Me**−**A**, the Si−N bonds lengthen (0.047−0.053 Å in **X**−**A** and 0.028 Å in **Me**−**A**). In addition, the C−C bonds become longer and the C−N bonds shorter indicating a greater degree of localization in the $(-NHCH)_2$ unit. When the methyl radical is added (**Me**−**A**), the C−C and C−N bond lengths show very little change, whereas the Si−CH_3 bond is long (1.923 Å) compared to other Si−C bonds. Electron

TABLE 1: Calculated Electronic Energies (hartrees), Zero-Point Energies (kcal/mol), Heat Capacity Corrections to 298 K (kcal/mol), Entropy (cal/mol·K) and Spin-Squared Values ($\langle S^2 \rangle$) Calculated at the B3LYP/SBS Level

	ZPC	C_p corr	S	$\langle S^2 \rangle$	B3LYP/SBS	B3LYP/LBS
A	41.9	3.4	67.6		−477.64745	−477.73632
AT[a]	40.6	3.9	74.6	2.01	−477.55314	−477.63895
CH_3	18.8	2.5	46.5	0.75	−39.84264	−39.85653
Me−A	64.1	5.0	82.9	0.76	−517.53588	−517.63997
Me−D	106.3	9.0	118.1	0.76	−995.19985	−995.39464
Me−TS	61.2	6.0	95.6	0.75	−517.49031	−517.59302
MeD−TS	106.3	8.7	122.3	0.76	−995.18501	−995.37706
$ClCH_3$	23.9	2.5	56.0		−500.11152	−500.15697
Cl−A	42.2	4.6	82.1	0.76	−937.86658	−937.98978
Cl−D	84.6	8.5	115.6	0.76	−1415.53326	−1415.74792
Cl−P1	65.9	6.0	90.0		−977.83386	−977.97601
Cl−P2	107.8	10.0	125.4		−1455.48668	−1455.71920
Cl−TS1	65.0	6.0	93.8		−977.67677	−977.81091
Cl−TS2	64.3	6.3	97.2		−977.67376	−977.81063
Cl−TS3	62.7	6.7	100.6	0.69	−977.70646	−977.84346
ClD−TS	84.6	8.2	115.8	0.76	−1415.51770	−1415.72991
ClA−TS	65.2	7.5	109.9	0.76	−1437.95702	−1438.13061
ClMeA−TS	87.3	7.9	112.3	0.76	−1017.63345	−1017.78579
ClMeD−TS	129.2	11.9	147.0	0.76	−1495.29462	−1495.53768
ClDCl−TS	107.5	11.4	143.3	0.76	−1915.62568	−1915.88940
$BrCH_3$	23.5	2.5	58.8		−2611.63240	−2614.07317
Br−A	42.1	4.7	85.0	0.76	−3049.39289	−3051.90445
Br−D	84.5	8.7	118.9	0.76	−3527.06051	−3529.66078
Br−P1	65.7	6.1	92.5		−3089.35807	−3091.88715
Br−P2	107.6	10.2	127.9		−3567.01446	−3569.63195
Br−TS1	64.8	6.1	95.7		−3089.20762	−3091.73264
Br−TS2	62.7	6.7	103.6	0.71	−3089.21634	−3091.74032
Br−TS3	61.2	7.5	111.8	1.00	−3089.23614	−3091.76072
BrD−TS	84.5	8.2	116.8	0.76	−3527.04677	−3529.64438
BrA−TS	64.7	7.6	114.5	0.76	−5661.02212	−5665.96792
BrMeA−TS	87.3	7.8	113.2	0.76	−3129.17238	−3131.71068
BrMeD−TS	129.1	12.0	148.4	0.76	−3606.83581	−3609.46322
ICH_3	23.2	2.6	60.8		−51.29691	−51.34492
I−A	42.1	4.8	87.6	0.76	−489.04402	−489.17480
I−D	84.5	8.7	120.9	0.76	−966.70179	−966.92838
I−P1	65.6	6.2	95.0		−529.00236	−529.15297
I−P2	107.7	10.2	129.5		−1006.65409	−1006.89921
I−TS1	64.6	6.2	98.4		−528.86767	−528.99464
I−TS2	62.4	6.9	107.3	0.82	−528.87552	−529.00960
ID−TS	84.3	8.4	121.3	0.76	−966.69006	−966.91470
IA−TS	63.9	8.0	120.9	0.78	−540.32671	−540.51151
IMeA−TS	86.9	8.0	116.1	0.77	−568.82684	−568.98773
IMeD−TS	128.9	12.0	148.8	0.77	−1046.48418	−1046.74062
CH_2Cl_2	18.6	2.8	64.6		−959.70053	−959.77776
$CHCl_3$	12.5	3.4	70.7		−1419.28431	−1419.39407
CCl_4	5.8	4.1	74.2		−1878.85980	−1879.00285
Cl2−TS	58.3	7.0	108.1	0.60	−1437.30515	−1437.47319
Cl3−TS	53.1	7.5	114.0	0.49	−1896.89944	−1897.09927
Cl4−TS	47.1	8.2	118.6	0.35	−2356.48627	−2356.71888
SiM	76.9	5.4	83.4		−556.26415	−556.26415
SiM−TS	97.6	8.9	119.5	0.67	−1056.32575	−1056.48006
SiM−Cl2TS	93.2	9.2	125.4	0.59	−1515.92477	−1516.11026

[a] Triplet silylene **A**.

donation from the methyl group strengthens the Si−N bonds and increases delocalization over the $(-NHCH)_2$ unit. On the other hand, the halogen atom withdraws electron density from the silicon atom and weakens (and lengthens) the Si−N bonds. The atomic NPA charges and spin densities of **X−A** and **Me−A** support this interpretation (Table 2). When a Cl or Br atom is attached to **A** (**Cl−A** or **Br−A**), the spin density is delocalized over the ring with very little spin density on the halogen atom, whereas, in contrast, the iodine atom has significant spin density in **I−A**. In **Me−A**, most of the spin density resides on silicon (0.62 e^-) due to 2c−2e Si−C bond formation and the prerequisite electron promotion.

The products from concerted oxidative addition of XCH_3, **X−P1**, (X = Cl, Br, I) show very similar ring geometries. All have a localized C−C double bond (1.348−1.349 Å) and C−N single bonds (1.416−1.418 Å). The Si−N bond lengths in the series **A** → **Cl−A** → **Cl−P1** vary irregularly, 1.779 → 1.832 → 1.739 Å. In **A**, the Si−N bonds are short due to π conjugation from nitrogen lone pairs into the empty silicon orbital, whereas in **Cl−P1** the Si−N bonds are short due to the stronger Si−N single bonds (more s character).

Relative electronic energies (ΔE), enthalpies at 0K (ΔH_{0K}), enthalpies at 298 K (ΔH_{298K}), and free energies at 298 K (ΔG_{298K}) of all stationary points relevant to the reaction pathways are tabulated in Tables 3−5. Bond enthalpies of X−C in XCH_3 and X−Si bond enthalpies in **X−A** and **X−P1** (X = Cl, Br, I) are given in Table 6. The X−C bond enthalpies of methyl halides are in good agreement with well-known experimental values.[33]

Bond formation in **X−A** can be viewed as somewhere between two extremes. At one end of the spectrum, 2c−2e bond formation takes place after electron promotion, whereas at the other end, 2c−3e bond formation takes place without electron promotion. The preferred mode depends on the required promotion energy versus the strength of the 2c−2e bond. The promotion energy in **A** can be estimated from the singlet−triplet energy gap (ΔH^{s-t}), which was calculated to be 60.3 kcal/mol (ΔH^{s-t}_{298}). Thus, the new 2c−2e bond energy must be greater than 60.3 kcal/mol; otherwise 2c−3e bonding will be favored. The Si−X bond strength in **X−P1** should be a good estimate of full intrinsic Si−X bond strength because no promotion energy is required. As shown in Table 6, the BDE_{298} of Si−Cl, Si−Br, and Si−CH_3 in **X−P1** is larger than ΔH^{s-t}_{298} but the BDE_{298} of Si−I is only slightly larger. Therefore, in **A**, where a promotion of 60.3 kcal/mol is required, the 2c−2e bond enthalpy of 65 kcal/mol is barely enough to form a 2c−2e bond in **I−A**. Indeed, the Si−I bond strength in **X−A** is only 20.1 kcal/mol and is characterized by a much longer Si−I bond than found in **I−P1** and a much higher spin density on iodine (Table 2). Both properties indicate that the Si−I bond in **I−A** may have significant 2c−3e character.

In the series X = Cl, Br, I, the Si−X bond enthalpies in **X−A** (52.5 < 37.8 < 20.1 kcal/mol) and **X−P1** (103.1 < 86.3 < 65.9 kcal/mol) follow similar trends. The former bond enthalpies (**X−A**) are 50.6, 48.5, and 45.8 kcal/mol smaller than the latter (**X−P1**) for X = Cl, Br, I, respectively, due to the required promotion energy in **A** (estimated from the singlet−triplet splitting as 60.3 kcal/mol), which must take place before a 2c−2e Si−X bond can form. On the other hand, the 2c−2e Si−X bond in **X−P1** can form without any additional promotion energy.

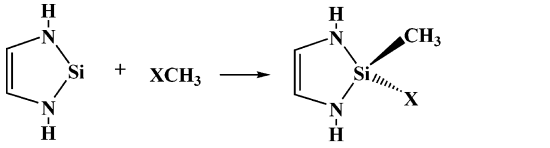

(1a)

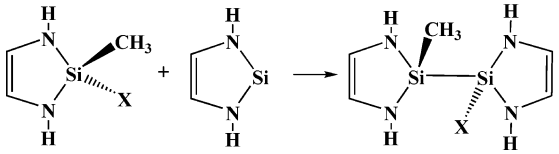

(1b)

In the currently proposed mechanism,[23] the first step in the reaction of XCH_3 with **A** is the concerted oxidative addition of XCH_3 (eq 1a). The monomer product observed when X = I, **X−P1**, would follow immediately. The dimer product, **X−P2**,

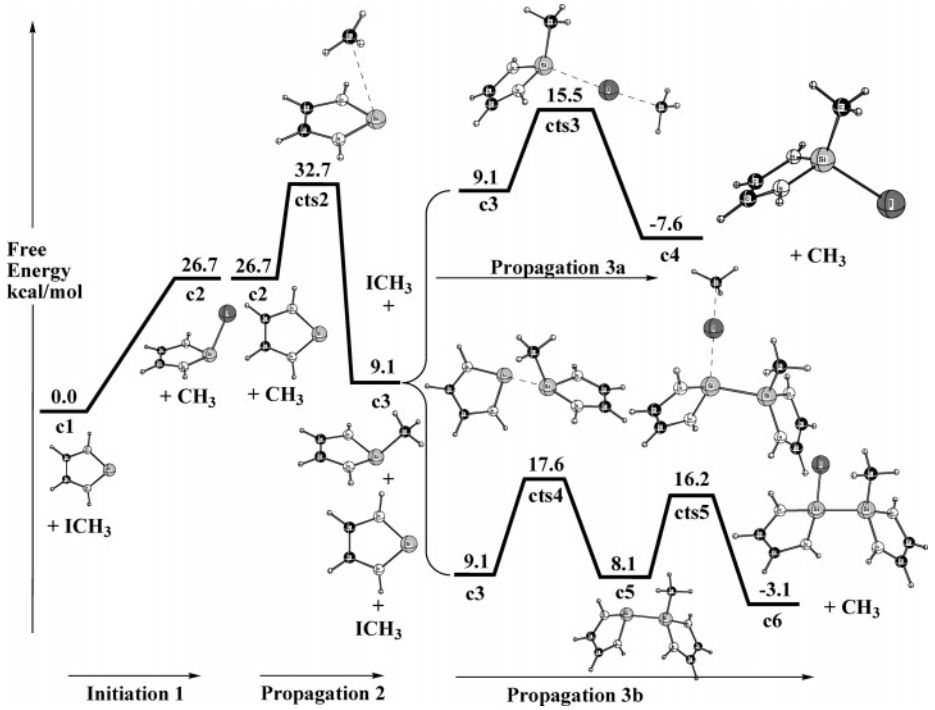

Figure 4. Schematic reaction free energy profile is presented for the reaction of **A** with ICH_3 at the B3LYP/LBS//B3LYP/SBS level. The initiation step of **A** + ICH_3 does not have a transition state.

follows from the insertion of **A** into the X−Si bond of **X**−**P1** (eq 1b). An alternative mechanism involving a dimer of **A** cannot occur because the dimer is not stable.[6]

The calculations below support a radical mechanism (eq 2−5). Free energy profiles in kcal/mol at 298 K are given in Figures 2-4 for X = Cl, Br, and I. The profile is divided into three sections, the initiation step (eq 2), the common propagation step (eq 3), and the competition between the two propagation steps (eqs 4 and 5), which lead to **X**−**P1** and **X**−**P2**, respectively.

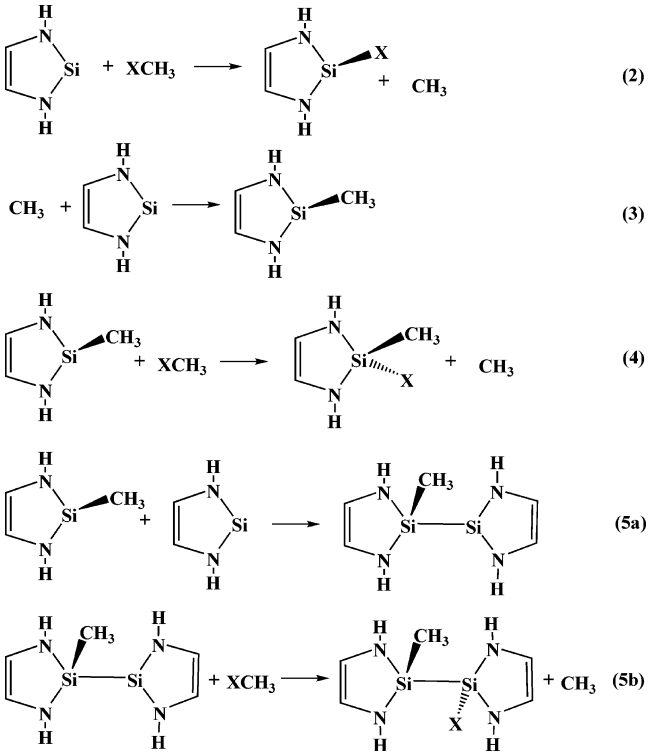

TABLE 2: Natural Atomic Charges (NPA) and Mulliken Spin Densities (MSD) of X−Si(NHCH)$_2$, (X = ep,[a] CH_3, Cl, Br, I) Radicals Calculated at the B3LYP/SBS Level

	Si		X		NH		CH		$(NHCH)_2$ [d]
	NPA	MSD	NPA	MSD	NPA	MSD	NPA	MSD	NPA
A	0.94	0.00			−0.60	0.00	0.13	0.00	−0.94
Me−**A**	1.26	0.62	−0.42[b]	−0.01[c]	−0.56	0.13	0.14	0.07	−0.84
Cl−**A**	1.11	0.33	−0.45	0.04	−0.51	0.20	0.18	0.14	−0.65
Br−**A**	1.04	0.29	−0.39	0.08	−0.51	0.19	0.18	0.14	−0.65
I−**A**	0.96	0.12	−0.32	0.24	−0.51	0.20	0.19	0.14	−0.65

[a] Electron pair, designating **A**. [b] Methyl group charge; atomic charges on methyl hydrogens are summed with charge on carbon. [c] Spin density on methyl carbon. [d] Ring −$(NHCH)_2$ group.

The concerted oxidative-addition barriers are compared with the lower-energy halogen-abstraction barriers in Table 7. The concerted transition states (**X**−**TS1** and **X**−**TS2**) have significantly higher free energies of activation than the halogen abstraction (**X**−**TS3**) free energy barrier. The latter barriers are 22.9, 16.0, and 22.8 kcal/mol lower in free energy than the concerted processes for X = Cl, Br, and I, respectively. In the case of iodine, a transition state for iodine abstraction could not be found. When X = Cl, Br, the activation free energy for halogen abstraction decreases (Table 8) whereas the reaction free energy increases. For X = I, the two trends meet, which explains why there is no transition state.

From the NBO analysis, there are three important donor−acceptor interactions in **X**−**TS1** and **X**−**TS2** (Table 9 and Figure 5). These are labeled **1**, **2**, and **3** and correspond to electron donation from the silicon lone pair (LP_{Si}) to the antibonding X−C orbital (σ^*_{X-C}), to electron donation from the lone pair orbital on X (LP_X) to the empty orbital on silicon (LP^*_{si}), and to electron donation from the X−C bonding orbital (σ_{X-C}) to the empty orbital on silicon (LP^*_{si}), respectively (Table 9). In **X**−**TS1**, the stable bis(amino)silylene is acting as the Lewis base, where interaction **1** is larger than **2**+**3**. The decrease of interaction **1** in **X**−**TS1** as **X** is changed from Cl to I (Cl 42.4 kcal/mol; Br 31.6 kcal/mol; I 25.1 kcal/mol) can be

TABLE 3: Relative Energies, Enthalpies, and Free Energies (kcal/mol) in the Reaction Profile for the Reaction of A with $ClCH_3$

label	species	ΔE_e	ΔH_{0K}	ΔH_{298K}	ΔG_{298K}
a1	$3\mathbf{A} + 2ClCH_3$	0.0	0.0	0.0	0.0
ats1	**Cl-TS3** + $2\mathbf{A}$ + $ClCH_3$	31.3	28.2	29.0	35.9
a2	**Cl−A** + CH_3 + $2\mathbf{A}$ + $ClCH_3$	29.5	24.7	26.0	24.5
ats2	**Me−TS** + **A** + $ClCH_3$ + **Cl−A**	29.4	25.1	26.5	30.5
a3	**Me−A** + **A** + $ClCH_3$ + **Cl−A**	−0.1[a]	−1.4	−1.0	6.9
ats3	**ClMeA-TS** + **A** + **Cl−A**	6.9	4.8	5.7	21.4
a4	**Cl−P1** + CH_3 + **A** + **Cl−A**	−22.4	−27.1	−25.7	−17.1
ats4	**MeD-TS** + $ClCH_3$ + **Cl−A**	−0.6[a]	−1.7	−0.8	15.4
a5	**Me−D** + $ClCH_3$ + **Cl−A**	−11.6	−12.8	−11.6	5.9
ats5	**ClMeD-TS** + **Cl−A**	−2.9	−4.9	−3.4	22.2
a6	**Cl−P2** + CH_3 + **Cl−A**	−26.7	−31.5	−29.3	−11.2

[a] Because the transition state is lower in energy than the reactant (**a3** → **ats4**), there must be an intervening intermediate. At the ΔE_e level, the **Me−A/A** complex is 2.7 kcal/mol more stable than **a3.**

TABLE 4: Relative Energies, Enthalpies, and Free Energies (kcal/mol) in the Reaction Profile for the Reaction of A with $BrCH_3$

label	species	ΔE_e	ΔH_{0K}	ΔH_{298K}	ΔG_{298K}
b1	$3\mathbf{A} + 2BrCH_3$	0.0	0.0	0.0	0.0
bts1	**Br−TS3** + $2\mathbf{A}$ + $BrCH_3$	30.6	26.4	28.0	32.3
b2	**Br−A** + CH_3 + $2\mathbf{A}$ + $BrCH_3$	30.4	25.8	27.2	25.7
bts2	**Me−TS** + **A** + $BrCH_3$ + **Br−A**	30.3	26.3	27.7	31.7
b3	**Me−A** + **A** + $BrCH_3$ + **Br−A**	0.9[a]	−0.3	0.3	8.0
bts3	**BrMeA-TS** + **A** + **Br−A**	2.4	1.0	1.7	18.0
b4	**Br−P1** + CH_3 + **A** + **Br−A**	−18.3	−22.6	−21.1	−12.5
bts4	**MeD-TS** + $BrCH_3$ + **Br−A**	0.4[a]	−0.5	0.4	16.6
b5	**Me−D** + $BrCH_3$ + **Br−A**	−10.6	−11.6	−10.4	7.0
bts5	**BrMeD-TS** + **Br−A**	−7.8	−9.3	−7.8	18.1
b6	**Br−P2** + CH_3 + **Br−A**	−23.6	−27.9	−25.7	−7.5

[a] Because the transition state is lower in energy than the reactant (**b3** → **bts4**), there must be an intervening intermediate. At the ΔE_e level, the **Me−A/A** complex is 2.7 kcal/mol more stable than **b3**.

TABLE 5: Relative Energies, Enthalpies, and Free Energies (kcal/mol) in the Reaction Profile for the Reaction of A with ICH_3

label	species	ΔE_e	ΔH_{0K}	ΔH_{298K}	ΔG_{298K}
c1	$3\mathbf{A} + 2ICH_3$	0.0	0.0	0.0	0.0
c2	**I−A** + CH_3 + $2\mathbf{A}$ + ICH_3	31.3	27.0	28.4	26.7
cts2	**Me−TS** + **A** + ICH_3 + **I−A**	31.2	27.4	28.9	32.7
c3	**Me−A** + **A** + ICH_3 + **I−A**	1.8[a]	0.9	1.5	9.1
cts3	**IMeA-TS** + **A** + **I−A**	0.0[a]	−1.3	−0.3	15.5
c4	**I−P1** + CH_3 + **A** + **I−A**	−13.7	−17.5	−15.9	−7.6
cts4	**MeD-TS** + ICH_3 + **I−A**	1.3[a]	0.7	1.6	17.6
c5	**Me−D** + ICH_3 + **I−A**	−9.8[a]	−10.4	−9.2	8.1
cts5	**IMeD-TS** + **I−A**	−10.4[a]	−11.6	−10.0	16.2
c6	**I−P2** + CH_3 + **I−A**	−19.9	−23.5	−21.3	−3.1

[a] Because the transition state is lower in energy than the reactant (**c3** → **cts3**, **c3** → **cts4**, and **c5** → **cts5**), there must be an intervening intermediate. At the ΔE_e level, the **Me−A**/ICH_3 complex is 1.8 kcal/mol more stable than **c3**; the **Me−A/A** complex is 2.7 kcal/mol more stable than **c3**; the **Me−D**/ICH_3 complex is 2.2 kcal/mol more stable than **c5**.

attributed to the destabilization of the X−C σ^* orbital, which reduces its acceptor ability. On the other hand, the stable bis(amino)silylene is acting as a Lewis acid in **X−TS2**, as shown by the combined interactions of **2** and **3** in which the acceptor orbital is LP^*_{si}. The largest interaction (**2** + **3**) occurs for X = Br (94.9 kcal/mol), followed by X = Cl (85.0 kcal/mol) and X = I (56.9 kcal/mol). Indeed, the lowest concerted free energy barrier for oxidative addition of XCH_3 to **A** occurs via **Br−TS2**. There has been extensive discussion in the literature about the increased Lewis basicity of **A** relative to dialkylsilylenes. However, in the concerted oxidative addition of XCH_3 to the

TABLE 6: Bond Dissociation Energies (BDE), Bond Dissociation Enthalpies at 0 K (BDE_0) and at 298 K (BDE_{298}) Calculated at the B3LYP/LBS//B3LYP/SBS Level (kcal/mol)

bond	BDE	BDE_0	BDE_{298}	ref[c]
$Cl-CH_3$	82.0	76.9	78.5	84.1[d]
$Br-CH_3$	68.2	63.5	65.0	70.0[d]
$I-CH_3$	51.5	47.1	48.5	56.6[d]
H_3C-Si[a]	29.6	26.1	26.9	
$Cl-Si$[a]	52.6	52.3	52.5	
$Br-Si$[a]	37.8	37.7	37.8	
$I-Si$[a]	20.2	20.1	20.1	
$Si-Cl$[b]	104.4	102.6	103.1	117.1 ± 2,[e] 98.9[f]
$Si-Br$[b]	87.4	85.8	86.3	101.6 ± 2,[e] 82.1[f]
$Si-I$[b]	67.0	65.5	65.9	82.2 ± 2,[e] 62.7[f]
$ClSi-CH_3$[b]	81.4	76.4	77.6	94.2 ± 1,[e] 70.5[f]
$BrSi-CH_3$[b]	79.2	74.3	75.5	
$ISi-CH_3$[b]	76.3	71.5	72.7	

[a] From **Me−A** and **X−A** (X = Cl, Br, I) radical species. [b] From **X−P1** (X = Cl, Br, I). [c] Literature values for BDE_{298}. [d] Reference 33. [e] BDE of Me_3Si-X (X = CH_3, Cl, Br, I), from ref 34. [f] Bond energy terms of Si−X (X = C, Cl, Br, I) derived from least-squares method. Reference 35.

TABLE 7: Comparison of Free Energies of Activation (kcal/mol) for Concerted Oxidative Addition with Halogen Abstraction Reaction for A + XCH_3

	X = Cl	X = Br	X = I
X−TS1[a]	60.0	57.0	63.1
X−TS2[a]	58.8	48.3	49.5
X−TS3[b]	35.9	32.3	26.7[c]

[a] Oxidative addition. [b] Halogen abstraction. [c] There is no transition state for halogen atom abstraction by **A** from ICH_3. The free energy of **I−A** plus CH_3 is 26.7 kcal/mol.

TABLE 8: Predicted Differences in Free Energies of Activation ($\Delta\Delta G_{298}$, kcal/mol) for Formation of CH_3 and I−Si Radical from $ClCH_3$ and $BrCH_3$ at B3LYP/LBS//B3LYP/SBS Level

X	X = Cl	X = Br	X = I
X−TS3	35.9	32.3	–
CH_3 + **X−A**	24.5	25.7	26.7
$\Delta(\Delta G_{298})$	11.4	6.6	~0.0

TABLE 9: Orbital Interaction Energies (kcal/mol) from Second Order Perturbation Theory Analysis in NBO Analysis at the HF/LBS Level

	orbital interaction		**Cl− TS1**	**Cl− TS2**	**Br− TS1**	**Br− TS2**	**I− TS1**	**I− TS2**
	donor	acceptor						
1[a]	LP_{Si}	σ^*_{X-C}[b]	42.4	58.1	31.6	13.0	25.1	40.1
2[a]	LP_X	LP^*_{Si}	0.4	62.6	0.4	43.1	0.3	21.1
3[a]	σ_{X-C} [b]	LP^*_{Si}	10.3	22.4	12.3	51.8	14.9	35.4

[a] For depiction of orbital interactions see Figure 5. [b] The σ and σ^* X−CH_3 bonds were defined by using CHOOSE and DEL keywords within the NBO analysis program.

stable bis(amino)silylene **A**, it appears that the silylene is still acting as the Lewis acid. It is interesting that the Lewis acid-Lewis base character of **A** can be captured by the two concerted transition states **X−TS1** and **X−TS2**. For X = Cl, the two transition states are separated by only 1.2 kcal/mol in free energy. This difference increases to 8.7 kcal/mol for X = Br and 13.6 kcal/mol for X = I. The increased separation between the two transition states (**X−TS1** and **X−TS2**) for X = I is likely due to the soft−soft acid−base character between iodine (soft base) and **A** (soft acid) in **I−TS2**. It must be emphasized that, though interesting from a pedagogical point of view, the concerted oxidative transition states, **X−TS1** and **X−TS2**, do not play a role in the reaction mechanism. For all three reactions,

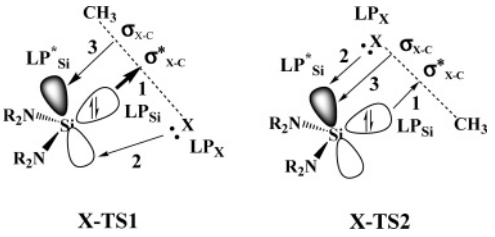

Figure 5. Orbital interactions are depicted that are analyzed by NBO in Table 9.

SCHEME 3

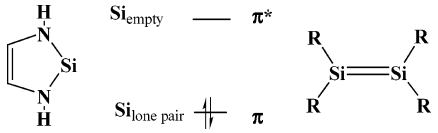

X = Cl, Br, and I, the halogen abstraction reaction, **X−TS3** is lower in free energy than the concerted oxidative addition (Table 7).

It has been reported that bis(amino)silylenes are electronically similar to trivalent phosphorus compounds (eqs 6 and 7),[17,37] because of strong π-conjugation. We suggest that a better

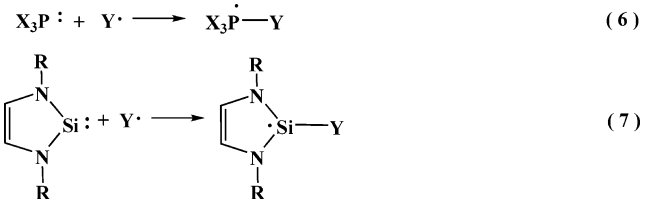

analogy might be disilenes, $R_2Si{=}SiR_2$ (Scheme 3). Kira has characterized the reaction of $R_2Si{=}SiR_2$ with R′X as proceeding through a "bimolecular abstraction mechanism".[13] In fact, in the reaction of $(i\text{-}Pr_3Si)_2Si{=}Si(i\text{-}Pr_3Si)_2$ with *t*-BuCl, the radical product is stable and has been identified by ESR.[38]

More supportive evidence for the analogue between bis(amino)silyene and disilene can be found from the nature of the transition state for halogen atom abstraction by both compounds. By comparing rate constants and exothermicities for the reactions of disilene with a series of chlorine- and bromine-containing molecules, it was concluded[13,38] that the transition states are "late" (silicon−halogen bond formation and halogen−carbon bond cleavage are well-advanced). In the reaction of bis(amino)silyene with halomethanes, the transitions state (**X−TS3**) are also "late" as judged by short forming Si−X and long breaking X−C bonds (Figure 1d,e). In contrast to the reactions of **A** (bis(amino)silyene) with XCH_3 that are "late", the reactions of **Me−A** with XCH_3 are "early", as judged by the long forming Si−X bonds and the short breaking X−C bonds in the transition states **XMeA-TS** (Figure 1d). Thus, the addition of the methyl substituent to **A** (**A** + CH_3 → **Me−A**) makes the halogen abstraction reactions much more exothermic and changes the transition states from "late" to "early".

The free energy barrier for halogen abstraction (forming two radical products) is clearly lower than the concerted oxidative addition barriers as illustrated in Table 7 for the three halomethanes considered, $ClCH_3$, $BrCH_3$, and ICH_3. In Figures 2−4, we present the free energies for the radical mechanism to **X−P1** and **X−P2**, X = Cl, Br, I.

In the initiation step, a halogen atom is abstracted by bis(amino)silylene (**A**), leaving behind a methyl radical. The methyl radical can react with another methyl radical to form ethane (chain terminating), react with the solvent (hexane or benzene) to form side products, react with XCH_3 in a degenerate reaction (CH_3 + X−CH_3 → CH_3−X + CH_3), or (much more likely) react with **A**. Reaction with **A** (labeled "Propagation 2"), a common step for all halomethanes, has a free energy barrier of 6.0 kcal/mol. The product, **Me−A**, can react with X−CH_3 ("Propagation 3a") or with another **A** ("Propagation 3b"). The competition between (3a) and (3b) will determine which products are formed. In the reaction of $ClCH_3$ with **A**, the two relevant free energies are "**ats3**" and "**ats5**", 21.4 and 22.2 kcal/mol. The calculation would predict a mixture of **Cl−P1** and **Cl−P2** because the free energy barriers are very similar.

In the chain mechanism, we depict the **Me−D** radical reacting with $ClCH_3$ to form **Cl−P2** plus CH_3 (Propagation 3b). In reality, there is the possibility that **Me−D** can react with another **A** to form **Me−T** ("**T**" for trimer). The free energy barrier for the **Me−D** + **A** → **Me−T** reaction is lower than for the **Me−D** + $ClCH_3$ → **Cl−P2** reaction (9.6 versus 16.3 kcal/mol), but the reaction is nonspontaneous by 5.9 kcal/mol.[39] When we consider that the experiments involve **1** with bulky *tert*-butyl groups on nitrogen rather than **A**, the possibility for forming the trimer adduct is even less likely.

This prediction agrees with experimental result where reaction of **1** with CCl_4 afforded a mixture of products.[14b] However, the only reported product of the reaction of **1** (not **A**) with CH_2Cl_2 or $CHCl_3$ (not $ClCH_3$) is the disilane product (**Cl−P2**). It should be noted that solvation effects in hexane or benzene (which have not been included in the present study) are expected to be small but could be large enough to affect the outcome of the reaction. Of course, the reaction can be "pushed" toward one product or the other by changing the initial $ClCH_3$:**A** ratio.

In the $BrCH_3$-containg pathway 3a (Figure 3, **Me−A** + $BrCH_3$), the transition state has a free energy of 18.0 kcal/mol, very similar to the free energy from pathway 3b (18.1 kcal/mol). The two pathways are expected (and found) to be competitive. In the ICH_3-containing pathway 3a (Figure 4, **Me−A** + ICH_3), the transition state has a smaller free energy than the pathway to disilane products (**I−P2**), 15.5 versus 17.6 kcal/mol. In addition, nonstatistical behavior (see below) may lead to the formation of **I−P1** by the capture of the CH_3 radical released in the initiation step.

It is very reasonable that the two barriers for addition of XCH_3 to **Me−A** or **Me−D** should be similar. In both transition states, the halogen atom is abstracted by a silicon atom in a similar chemical environment. For **Me−A** + XCH_3, the substituent on the trivalent silicon is methyl whereas in **Me−D** + XCH_3, the substituent is methyl-bis(amino)silylene.

We also explored the fate of **X−A**, which should lead to minor products, perhaps below the detection limit in the experimental studies. The reaction of **X−A** with **A** has free energy barriers of 8.3, 9.0, and 8.4 kcal/mol for X = Cl, Br, and I (for structures see: **XD−TS**, Figure 1). In analogy with **Me−D**, the most likely reaction of **Cl−D** is with $ClCH_3$ to give the dichloro version of the disilane product. The free energy barrier for this reaction is 17.5 kcal/mol (Figure 1e). The alternative reactions of **X−A** are with XCH_3, which have free energy barriers of 18.0, 14.4, and 12.6 kcal/mol for X = Cl, Br, and I, respectively, to form the dihalogen version of **X−P1** (Figure 1e). Thus, there may be dihalogen products produced (i.e., two halogens on **X−P1** and **X−P2**) in the reaction of XCH_3 + **A**, but the concentrations may be low because **X−A** is only generated in the initiation step.

One shortcoming of our model is that the free energy barriers for the initiation steps are still too high to explain the experimental observation where the reactions proceed at room

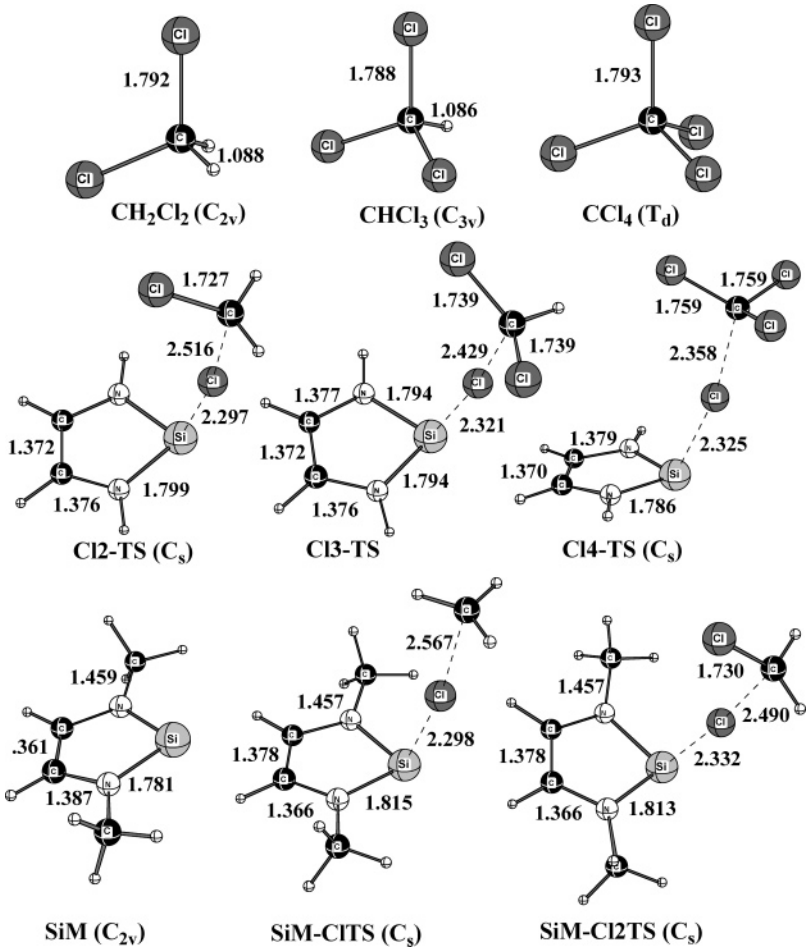

Figure 6. Geometries (B3LYP/6-31+G(d)) of reactants CH_2Cl_2, $CHCl_3$, and CCl_4 and the transition states for the initiation steps (chlorine atom abstraction by **A**) **Cl2−TS**, **Cl3−TS**, and **Cl4−TS**. In addition, geometry of reactant **SiM** and the transition states for the initiation steps (chlorine atom abstraction by **SiM**) **SiM−ClTS** and **SiM−Cl2TS**.

TABLE 10: Comparison of Activation Energies, Enthalpies, and Free Energies (kcal/mol) in the Initiation Steps for the Reaction of A with $ClCH_3$, CH_2Cl_2, $CHCl_3$ or CCl_4 and for the Reaction of SiM with $ClCH_3$ and CH_2Cl_2

	ΔE_e	ΔH_{0K}	ΔH_{298K}	ΔG_{298K}
Cl-TS3	31.3	28.2	29.0	35.9
Cl2-TS	25.7	23.5	24.3	31.5
Cl3-TS	19.5	18.2	19.0	26.2
Cl4-TS	12.7	12.1	12.8	19.8
SiM-ClTS	30.0	26.8	27.9	33.8
SiM-Cl2TS	24.1	21.8	22.8	29.6

temperature. This can be explained by the fact that our model system is not the same as the observed reaction. Most of the reported reactions are those of stable silylene **1** with CH_2Cl_2, $CHCl_3$, and CCl_4. Therefore, the effect of additional halogen atoms on the entering methyl carbon was examined in the reaction of **A** with CH_2Cl_2, $CHCl_3$, and CCl_4, as well as the effect of additional methyl groups on the ring nitrogen atoms in the silylene (i.e., N,N′-dimethyl derivative, **SiM**) in the reaction with $ClCH_3$. In addition, to confirm the additivity of these effects, an investigation of the reaction of **SiM** with CH_2Cl_2 was also carried out. Optimized geometries of the reactants and transition states are given in Figure 6, and the calculated activation barriers are tabulated in Table 10. The additional halogens on the methyl group lower the activation free energy barrier by about 5 kcal/mol per chlorine ($CH_{4-n}Cl_n$: $n = 1-4$; $\Delta G^{\ddagger}_{298K} = 35.9$, 31.5, 26.2, 19.9 kcal/mol, respectively). The lowering of the free energy barriers can be attributed to the stabilizing effect of the chlorine on the forming methyl radical.

Two methyl substituents on the ring nitrogen atoms cause the activation free energy barrier to be lower by about 2 kcal/mol. The electron donation from the methyl groups to the bis(amino)silylene ring enhances the electron delocalization over the five-member ring system and stabilizes the transition state. The two effects (methyl groups on nitrogen and additional chlorine atoms on carbon) are additive and the activation free energy barrier for the reaction of **SiM** with CH_2Cl_2 ($\Delta G^{\ddagger}_{298K} = 29.6$ kcal/mol) is 6.3 kcal/mol lower than that of the model reaction. Thus, if we consider the stable silylene **1** reacting with CH_2Cl_2, $CHCl_3$, or CCl_4, the initiation free energy barriers might be reasonable for a reaction that occurs at room temperature.

One experimental peculiarity of the RCl + **A** reaction is that R = *t*-Bu and R = $CHCl_2$ lead to different products. $CHCl_3$ leads to **Cl−P2** (with a $CHCl_2$ substituent rather than CH_3), *t*-BuCl leads to the corresponding **Cl−P1** product, the same product observed with ICH_3. We think the answer to this riddle may come from nonstatistical kinetic models.[40] In the transition state for the initiation step, the transition vector (231i cm^{-1}) is a Cl−CH_3 bond stretch (Figure 7). The radical products are 3.0 kcal/mol lower in enthalpy (Table 1) than the transition state and the excess energy will become kinetic energies of two separating species such that the methyl radical will leave the vicinity of the **Cl−A** radical. If the reaction of *t*-BuCl follows a similar path, the 3.0 kcal/mol of enthalpy may be absorbed

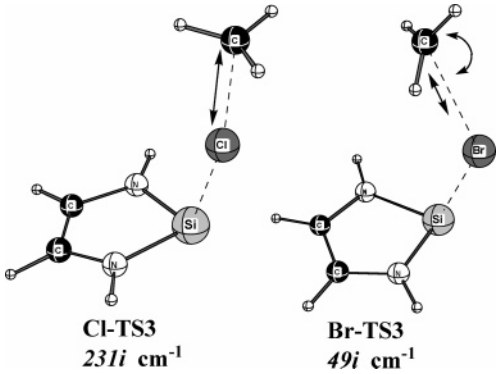

Figure 7. Transition vectors of the two transition states (**Cl−TS3** and **Br−TS3**) that indicate the ejection of a methyl radical during halogen abstraction. A transition state does not exist in the abstraction of iodine from ICH_3 by **A**.

by vibrations of the *t*-Bu group such that the *t*-Bu group may not depart the vicinity of **Cl−A** and be captured to form the corresponding **Cl−P1** product.

Another reason R = *t*-Bu leads to the monomer is due to steric congestion in the transition state for formation of the dimer. In the case of *t*-BuCl reacting with **1** there are five *t*-Bu groups in the transition state (**MeD-TS**) with significant crowding between the two units. In this case, there is an advantage of propagation step 3a over 3b.

Conclusion

The present calculations of the reaction of bis(amino)silylene with halomethane indicate a radical reaction mechanism rather than a concerted oxidative addition of the halomethane. The free energies of activation for the radical mechanism are 16 to 23 kcal/mol lower than for the concerted pathway. The chain pathway includes the initiation step, which produces a halogen-addition product and a methyl radical, and propagation steps, which consume one methyl radical and produce one methyl radical. The monomer and dimer products from the halomethane addition arise from the competition between two propagation steps. In one pathway, the halomethane adds to the methyl-bis-(amino)silylene radical (**Me−A**), whereas in the competing pathway, the methyl-bis(amino)silylene radical first reacts with another bis(amino)silylene, which, in turns, reacts with halomethane to abstract a halogen atom. Because the competing pathways are within a few kcal/mol of each other, secondary effects (such as solvation) may have decisive roles in determining the outcome of the reaction.

The observation that $CHCl_3$ and *t*-BuCl lead to different products can be explained within the present mechanism if nonstatisical effects are important. The large manifold of vibrational modes in the *t*-Bu radical may couple efficiently with the transition vector allowing the *t*-Bu radical to be "captured" in a single reaction step. A complete understanding of the reaction mechanism may require trajectory studies of branching propagation steps. However, these studies are beyond the scope of the present work.

Acknowledgment. Computer time was made available on the Auburn COSAM PRISM cluster. We thank Professor Bob West for valuable suggestions.

Supporting Information Available: Cartesian coordinates of all optimized structures in Table 1 at the B3LYP/6-31+G(d) level are given in Table S1. This material is available free of charge via the Internet at http://pubs.acs.org.

References and Notes

(1) Denk, M.; Lennon, R.; Hayashi, R.; West, R.; Belyakov, A. V.; Verne, H. P.; Haaland, A.; Wagner, M.; Metzler, N. *J. Am. Chem. Soc.* **1994**, *116*, 2691.

(2) (a) Heinemann, C.; Müller, T.; Apeloig, Y.; Schwarz, H. *J. Am. Chem. Soc.* **1996**, *118*, 2023. (b) Veszprémi, T.; Nyulászi, L.; Jajgató, B.; Heinicke, J. *THEOCHEM* **1998**, *431*, 1.

(3) (a) Boehme, C.; Frenking, G. *J. Am. Chem. Soc.* **1996**, *118*, 2039. (b) Boehme, C.; Frenking, G. *Organometallics* **1998**, *17*, 5801.

(4) Heinemann, C.; Herrmann, W. A.; Thiel, W. *J. Organomet. Chem.* **1994**, *475*, 73.

(5) West, R.; Buffy, J. J.; Haaf, M.; Müller, T.; Gehrhus, B.; Lappert, M. F.; Apeloig, Y. *J. Am. Chem. Soc.* **1998**, *120*, 1639.

(6) Oláh, J.; Veszprémi, T. *J. Organomet. Chem.* **2003**, *686*, 112.

(7) (a) Apeloig, Y.; Karni, M. In *The Chemistry of Organic Silicon Compounds*; Rappoport, Z., Apeloig, Y., Eds.; Wiley: New York, 1998; Vol. 2. Part 1, p 1. (b) Tokitoh, N. *Acc. Chem. Res.* **2004**, *37*, 86.

(8) (a) Arduengo, A. J., III; Bock, H.; Chen, H.; Denk, M.; Dixon, D. A.; Green, J. C.; Herrmann, W. A.; Jones, N. L.; Wagner, M.; West, R. *J. Am. Chem. Soc.* **1994**, *116*, 6641. (b) Denk, M.; Green, J. C.; Metzler, N.; Wagner, M. *J. Chem. Soc., Dalton Trans.* **1994**, 2405. (c) Blakeman, P.; Gehrhus, B.; Green, J. C.; Heinicke, J.; Lappert, M. F.; Kindermann, M.; Veszprémi, T. *J. Chem. Soc., Dalton Trans.* **1996**, 1475. (d) Pause, L.; Robert, M.; Heinicke, J.; Kühl, O. *J. Chem. Soc., Perkin Trans. 2* **2001**, 1383. (e) Dhiman, A.; Müller, T.; West, R.; Becker, J. Y. *Organometallics* **2004**, *23*, 5689. (f) Hill, N. J.; West, R. *J. Organomet. Chem.*, **2004**, *689*, 4165.

(9) Urquhart, S. G.; Hitchcock, A. P.; Lehmann, J. F.; Denk, M. *Organometallics* **1998**, *17*, 2352.

(10) (a) Lehmann, J. F.; Urquhart, S. G.; Ennis, L. E.; Hitchcock, A. P.; Hatano, K.; Gupta, S.; Denk, M. K. *Organometallics* **1999**, *18*, 1862. (b) Naka, A.; Hill, N. J.; West, R. *Organometallics* **2004**, *23*, 6330.

(11) Leites, L. A.; Bukalov, S. S.; Denk, M.; West, R.; Haaf, M. *J. Mol. Struct.* **2000**, *550*, 329.

(12) Gaspar, P. P.; West, R. In *The Chemistry of Organic Silicon Compounds*; Rappoport, Z., Apeloig, Y., Eds.; Wiley: New York, 1998; Vol. 2, Part 3, p 2463.

(13) (a) Kira, M. *Pure Appl. Chem.* **2000**, *72*, 2333. (b) Kira, M. *J. Organomet. Chem.* **2004**, *689*, 4475.

(14) (a) Gehrhus, B.; Lappert, M. F. *J. Organomet. Chem.* **2001**, *617*, 209. (b) Haaf, M.; Schmedake, T. A.; West, R. *Acc. Chem. Res.* **2000**, *33*, 704. (c) Tokitoh, N.; Okazaki, R. *Coord. Chem. Rev.* **2000**, *210*, 251.

(15) Amoroso, D.; Haaf, M.; Yap, G. P. A.; West, R.; Fogg, D. E. *Organometallics* **2002**, *21*, 534.

(16) Avent, A. G.; Gehrhus, B.; Hitchcock, P. B.; Lappert, M. F.; Maciejewski, H. *J. Organomet. Chem.* **2003**, *686*, 321.

(17) Schmedake, T. A.; Haaf, M.; Paradise, B. J.; Millevolte, A. J.; Powell, D. R.; West, R. *J. Organomet. Chem.* **2001**, *636*, 17.

(18) Haaf, M.; Schmedake, T. A.; Paradise, B. J.; West, R. *Can. J. Chem.* **2000**, *78*, 1526.

(19) (a) *Carbene Chemistry: from fleeting intermediates to powerful reagents*; Bertrand, G., Ed.; Marcel Dekker: New York, 2002. (b) *Reactive Intermediate Chemistry*; Moss, R. A., Platz, M. S., Jones, M., Jr., Eds.; Wiley-Interscience: Hoboken, NJ, 2004.

(20) Ishida, S.; Iwamoto, T.; Kabuto, C.; Kira, M. *Chem. Lett.* **2001**, 1102.

(21) Haaf, M.; Schmiedl, A.; Schmedake, T. A.; Powell, D. R.; Millevolte, A. J.; Denk, M.; West, R. *J. Am. Chem. Soc.* **1998**, *120*, 12714.

(22) Moser, D. F.; Bosse, T.; Olson, J.; Moser, J. L.; Guzei, I. A.; West, R. *J. Am. Chem. Soc.* **2002**, *124*, 4186.

(23) (a) Su, M.-D. *J. Am. Chem. Soc.* **2003**, *125*, 1714. (b) Su, M.-D. *Chem. Phys. Lett.* **2003**, *374*, 385.

(24) Koch, W.; Holthausen, M. C. *A Chemist's Guide to Density Functional Theory*; Wiley: New York, 2001.

(25) Frisch, M. J.; Trucks, G. W.; Schlegel, H. B.; Scuseria, G. E.; Robb, M. A.; Cheeseman, J. R.; Montgomery, J. A., Jr.; Vreven, T.; Kudin, K. N.; Burant, J. C.; Millam, J. M.; Iyengar, S. S.; Tomasi, J.; Barone, V.; Mennucci, B.; Cossi, M.; Scalmani, G.; Rega, N.; Petersson, G. A.; Nakatsuji, H.; Hada, M.; Ehara, M.; Toyota, K.; Fukuda, R.; Hasegawa, J.; Ishida, M.; Nakajima, T.; Honda, Y.; Kitao, O.; Nakai, H.; Klene, M.; Li, X.; Knox, J. E.; Hratchian, H. P.; Cross, J. B.; Adamo, C.; Jaramillo, J.; Gomperts, R.; Stratmann, R. E.; Yazyev, O.; Austin, A. J.; Cammi, R.; Pomelli, C.; Ochterski, J. W.; Ayala, P. Y.; Morokuma, K.; Voth, G. A.; Salvador, P.; Dannenberg, J. J.; Zakrzewski, V. G.; Dapprich, S.; Daniels, A. D.; Strain, M. C.; Farkas, O.; Malick, D. K.; Rabuck, A. D.; Raghavachari, K.; Foresman, J. B.; Ortiz, J. V.; Cui, Q.; Baboul, A. G.; Clifford, S.; Cioslowski, J.; Stefanov, B. B.; Liu, G.; Liashenko, A.; Piskorz, P.; Komaromi, I.; Martin, R. L.; Fox, D. J.; Keith, T.; Al-Laham, M. A.; Peng, C. Y.; Nanayakkara, A.; Challacombe, M.; Gill, P. M. W.; Johnson,

B.; Chen, W.; Wong, M. W.; Gonzalez, C.; Pople, J. A. *Gaussian03*, Revision B.4; Gaussian, Inc.: Pittsburgh, PA, 2003.

(26) (a) Becke, A. D. *J. Chem. Phys.* **1993**, *98*, 5648. (b) Lee, C.; Yang, W.; Parr, R. G. *Phys. Rev. B* **1988**, *37*, 785. (c) Miehlich, B.; Savin, A.; Stoll, H.; Preuss, H. *Chem. Phys. Lett.* **1989**, *157*, 200.

(27) (a) Hay, P. J.; Wadt, W. R. *J. Chem. Phys.* **1985**, *82*, 270. (b) Wadt, W. R.; Hay, P. J. *J. Chem. Phys.* **1985**, *82*, 284. (c) Hay, P. J.; Wadt, W. R. *J. Chem. Phys.* **1985**, *82*, 299.

(28) *MOLDEN*, Schaftenaar, G.; Noordik, J. H. *J. Comput.-Aided Mol. Design* **2000**, *14*, 123.

(29) (a) Gonzalez, C.; Schlegel, H. B. *J. Chem. Phys.* **1989**, *90*, 2154. (b) Gonzalez, C.; Schlegel, H. B. *J. Phys. Chem.* **1990**, *94*, 5523.

(30) Dolg, M.; Stoll, H.; Preuss, H.; Pitzer, R. M. *J. Phys. Chem.* **1993**, *97*, 5852.

(31) Reed, A.; Curtiss, L. A.; Weinhold, F. *Chem. Rev.* **1988**, *88*, 899.

(32) Becker, J. S.; Staples, R. J.; Gordon, R. G. *Cryst. Res. Technol.* **2004**, *39*, 85.

(33) James, A.; Lord, M. *VNR Index of Chemical and Physical Data*; Van Nostrand Reinhold: New York, 1992; p 485.

(34) Becerra, R.; Walsh, R. In *The Chemistry of Organic Silicon Compounds*; Rappoport, Z., Apeloig, Y., Eds.; Wiley: New York, 1998; Vol. 2, Part 1, p 153.

(35) Leroy, G.; Temsamani, D. R.; Wilante, C. *THEOCHEM* **1994**, *306*, 21.

(36) Metrangolo, P.; Resnati, G. In *Encyclopedia of Supramolecular Chemistry*; Atwood, J. L., Steed, J. W., Eds.; Marcel Dekker: New York, 2004; p 628.

(37) Tumanskii, B.; Pine, P.; Apeloig, Y.; Hill, N. J.; West, R. *J. Am. Chem. Soc.* **2002**, *124*, 7786.

(38) Kira, M.; Ishima, T.; Iwamoto, T.; Ichinohe, M. *J. Am. Chem. Soc.* **2001**, *123*, 1676.

(39) The free energy barrier for **Me**−**D** + **A** → **Me**−**T** is lower than the free energy barrier for **Me**−**D** + $BrCH_3$ → **Br**−**P2** (9.6 versus 11.1 kcal/mol) but the free energy of reaction is less spontaneous (5.9 versus −14.5 kcal/mol). The free energy barrier for **Me**−**D** + **A** → **Me**−**T** is higher than the free energy barrier for **Me**−**D** + ICH_3 → **I**−**P2** (9.6 versus 8.1 kcal/mol) and the free energy of reaction is less spontaneous (5.9 versus −11.2 kcal/mol).

(40) (a) Carpenter, B. K. In *Reactive Intermediate Chemistry*; Moss, R. A., Platz, M. S., Jones, M., Jr., Eds.; Wiley-Interscience: New York, 2004; p 925. (b) Carpenter, B. K. *Angew. Chem., Int. Ed. Engl.* **1998**, *37*, 3340. (c) Nummela, J. A.; Carpenter, B. K. *J. Am. Chem. Soc.* **2002**, *124*, 8512. (d) Carpenter, B. K. *J. Am. Chem. Soc.* **1995**, *117*, 6336. (e) Carpenter, B. K. *Acc. Chem. Res.* **1992**, *25*, 520.